



جامعة الملك عبد الله  
للعلوم والتقنية  
King Abdullah University of  
Science and Technology

## Highly Stable Aqueous Zinc-ion Storage Using Layered Calcium Vanadium Oxide Bronze Cathode

Item Type	Article
Authors	Xia, Chuan; Guo, Jing; Li, Peng; Zhang, Xixiang; Alshareef, Husam N.
Citation	Xia C, Guo J, Li P, Zhang X, Alshareef HN (2018) Highly Stable Aqueous Zinc-ion Storage Using Layered Calcium Vanadium Oxide Bronze Cathode. Angewandte Chemie International Edition. Available: <a href="http://dx.doi.org/10.1002/anie.201713291">http://dx.doi.org/10.1002/anie.201713291</a> .
Eprint version	Post-print
DOI	<a href="https://doi.org/10.1002/anie.201713291">10.1002/anie.201713291</a>
Publisher	Wiley
Journal	Angewandte Chemie
Rights	This is the peer reviewed version of the following article: Highly Stable Aqueous Zinc-ion Storage Using Layered Calcium Vanadium Oxide Bronze Cathode, which has been published in final form at <a href="http://doi.org/10.1002/anie.201713291">http://doi.org/10.1002/anie.201713291</a> . This article may be used for non-commercial purposes in accordance With Wiley Terms and Conditions for self-archiving.
Download date	05/08/2022 07:08:51
Link to Item	<a href="http://hdl.handle.net/10754/627133">http://hdl.handle.net/10754/627133</a>

## Accepted Article

**Title:** Highly Stable Aqueous Zinc-ion Storage Using Layered Calcium Vanadium Oxide Bronze Cathode

**Authors:** Chuan Xia, Jing Guo, Peng Li, Xixiang Zhang, and Husam N. Alshareef

This manuscript has been accepted after peer review and appears as an Accepted Article online prior to editing, proofing, and formal publication of the final Version of Record (VoR). This work is currently citable by using the Digital Object Identifier (DOI) given below. The VoR will be published online in Early View as soon as possible and may be different to this Accepted Article as a result of editing. Readers should obtain the VoR from the journal website shown below when it is published to ensure accuracy of information. The authors are responsible for the content of this Accepted Article.

**To be cited as:** *Angew. Chem. Int. Ed.* 10.1002/anie.201713291  
*Angew. Chem.* 10.1002/ange.201713291

**Link to VoR:** <http://dx.doi.org/10.1002/anie.201713291>  
<http://dx.doi.org/10.1002/ange.201713291>

## COMMUNICATION

## Highly Stable Aqueous Zinc-ion Storage Using Layered Calcium Vanadium Oxide Bronze Cathode

Chuan Xia,<sup>†</sup> Jing Guo,<sup>†</sup> Peng Li, Xixiang Zhang and Husam N. Alshareef\*

**Abstract:** Cost-effective aqueous rechargeable batteries are attractive alternatives to non-aqueous cells for stationary grid energy storage. Among different aqueous cells, zinc-ion batteries (ZIBs), based on  $\text{Zn}^{2+}$  intercalation chemistry, stand out as they can employ high-capacity Zn metal as anode material. Herein, we report a layered calcium vanadium oxide bronze as cathode material for aqueous Zn batteries. For the storage of  $\text{Zn}^{2+}$  ions in aqueous electrolyte, we demonstrate that calcium based bronze structure can deliver a high capacity of  $340 \text{ mAh g}^{-1}$  at  $0.2 \text{ C}$ , good rate capability and very long cycling life (96% retention after 3000 cycles at  $80 \text{ C}$ ). Further, we investigate the  $\text{Zn}^{2+}$  storage mechanism, and the corresponding electrochemical kinetics in this bronze cathode. Finally, we show that our Zn cell delivers an energy density of  $267 \text{ Wh kg}^{-1}$  at a power density of  $53.4 \text{ W kg}^{-1}$ .

Aqueous rechargeable batteries are a promising class of batteries for grid-scale electrochemical energy storage.<sup>[1]</sup> This is largely because of their low-cost and operational safety. Further, it is well known that aqueous electrolytes offer much higher ionic conductivities ( $\approx 1 \text{ S cm}^{-1}$ ), compared to non-aqueous electrolytes ( $\approx 1\text{--}10 \text{ mS cm}^{-1}$ ), which favors high-rate capabilities.<sup>[2]</sup> Efforts in large-scale aqueous energy storage has spanned naturally abundant  $\text{Na}^+$  and  $\text{K}^+$  intercalation materials,<sup>[3]</sup> as well as multivalent charge carriers (e.g.,  $\text{Zn}^{2+}$ ,  $\text{Ca}^{2+}$ ,  $\text{Mg}^{2+}$ , and  $\text{Al}^{3+}$ ).<sup>[4]</sup> Obviously, rechargeable cells employing multivalent ions can, in principle, deliver higher storage capacity due to multiple electron transfers. Among them, aqueous zinc-ion batteries (ZIBs), based on  $\text{Zn}^{2+}$  intercalation chemistry, stand out owing to the following properties of Zn anode: 1) high capacity ( $820 \text{ mAh g}^{-1}$ ;  $5851 \text{ mAh mL}^{-1}$ ); 2) high-abundance, and low-cost;<sup>[1b]</sup> 3) low redox potential ( $-0.76 \text{ V}$  vs standard hydrogen electrode);<sup>[5]</sup> and 4) impressive electrochemical stability in water due to a high overpotential for hydrogen evolution.<sup>[2]</sup> Moreover, replacement of the alkaline electrolyte by mild neutral pH (or slightly acidic) solution can virtually eliminate the dendritic zinc issues, which prevail in alkaline zinc cells; and simultaneously decrease the environmental impact and maintenance cost.<sup>[6]</sup> One of the main challenges which hinder the practical application of aqueous ZIBs is the lack of suitable intercalation cathodes, which can offer high capacity and good structure stability during  $\text{Zn}^{2+}$  (de)intercalation.

Thus, the development of high performance ZIB cathode is a prerequisite to achieve stable aqueous zinc-ion storage.

In the early stages of development, polymorphous of  $\text{MnO}_2$  were seriously investigated as potential  $\text{Zn}^{2+}$  host materials.<sup>[1a, 7]</sup> Afterwards, Prussian blue analogs were proposed to realize stable aqueous ZIBs.<sup>[8]</sup> Unfortunately, these electrodes suffer from either limited capacity or very poor cycling stability. Very recently, layered and hydrated  $\text{V}_2\text{O}_5$  derivatives (e.g.  $\text{Zn}_{0.25}\text{V}_2\text{O}_5 \cdot n\text{H}_2\text{O}$ )<sup>[2]</sup> were reported as high-performance ZIB cathodes, which delivered high capacity ( $>300 \text{ mAh g}^{-1}$ ) and long-term cycling stability ( $>1000$  cycles), as well as impressive rate capability. Such performance improvements were mainly attributed to the following reasons: 1) their open-framework crystal structure which has pillars between  $\text{V}_2\text{O}_5$  bilayers (leading to expanded interlayer spacing), which insures fast and reversible  $\text{Zn}^{2+}$  insertion/removal. In addition, compared with monovalent alkali metal cations (e.g.  $\text{Li}^+$ ,  $\text{Na}^+$ ,  $\text{K}^+$ ), the divalent metal ions bonded with oxygen atoms can bring about stronger ionic bonds,<sup>[9]</sup> better binding of the layers together, which effectively prevents structural collapse; 2) the tendency of vanadium to exist in multiple oxidation states, hence making it high-capacity in principle; 3) the charge shield effect of the crystal  $\text{H}_2\text{O}$ , which could reduce the effective charges of intercalated  $\text{Zn}^{2+}$  ions, and thus enhance the capacity and rate performance.<sup>[6, 10]</sup> To capitalize on these features, herein, we propose double-layered calcium vanadium oxide bronze ( $\text{Ca}_{0.25}\text{V}_2\text{O}_5 \cdot n\text{H}_2\text{O}$  or CVO) as more suitable aqueous ZIB intercalation cathode compared to  $\text{Zn}_{0.25}\text{V}_2\text{O}_5 \cdot n\text{H}_2\text{O}$  for the following considerations: 1) compared to  $\text{ZnO}_6$  octahedra pillars in  $\text{Zn}_{0.25}\text{V}_2\text{O}_5 \cdot n\text{H}_2\text{O}$  compound, the larger  $\text{CaO}_7$  polyhedra in CVO may further expand the cavity size between  $\text{V}_4\text{O}_{10}$  layers; 2) the smaller molecular weight and density of CVO probably can give higher gravimetric and volumetric capacity; 3) the CVO offer 4-folds higher electrical conductivity than  $\text{Zn}_{0.25}\text{V}_2\text{O}_5 \cdot n\text{H}_2\text{O}$ , as demonstrated later. We show that freestanding CVO paper cathode deliver capacities of  $340$  and  $289 \text{ mAh g}^{-1}$  at  $0.2$  and  $1 \text{ C}$ , respectively. The fast electrochemical kinetics of CVO is also quantitatively illustrated using cyclic voltammetry. We demonstrate that, even when cycled at  $80 \text{ C}$ , the CVO cathode retain  $\approx 96\%$  and  $\approx 78\%$  of its initial capacity after 3000 and 5000 cycles, respectively. A highly reversible  $\text{Zn}^{2+}$  intercalation mechanism is elucidated using *ex-situ* X-ray diffraction (XRD), X-ray photoelectron spectroscopy (XPS) and transmission electron microscope (TEM) studies.

The CVO sample was synthesized using a one-step hydrothermal method (see supporting information for details). As shown in **Fig. 1a** and supporting **Fig. S1**, the crystal structure of CVO is very similar as  $\delta$ -type  $\text{Zn}_{0.25}\text{V}_2\text{O}_5 \cdot n\text{H}_2\text{O}$ .<sup>[11]</sup> Both of these oxides can be described in a common manner where  $\text{V}_2\text{O}_5$  layers stack along

[\*] C. Xia, J. Guo, Dr. P. Li, Prof. X.X. Zhang, Prof. H.N. Alshareef  
Materials Science and Engineering  
King Abdullah University of Science and Technology (KAUST)  
Thuwal 23955-6900, Saudi Arabia  
E-mail: husam.alshareef@kaust.edu.sa

[†] These authors contributed equally to this work

Supporting information for this article is given via a link at the end of the document.

## COMMUNICATION

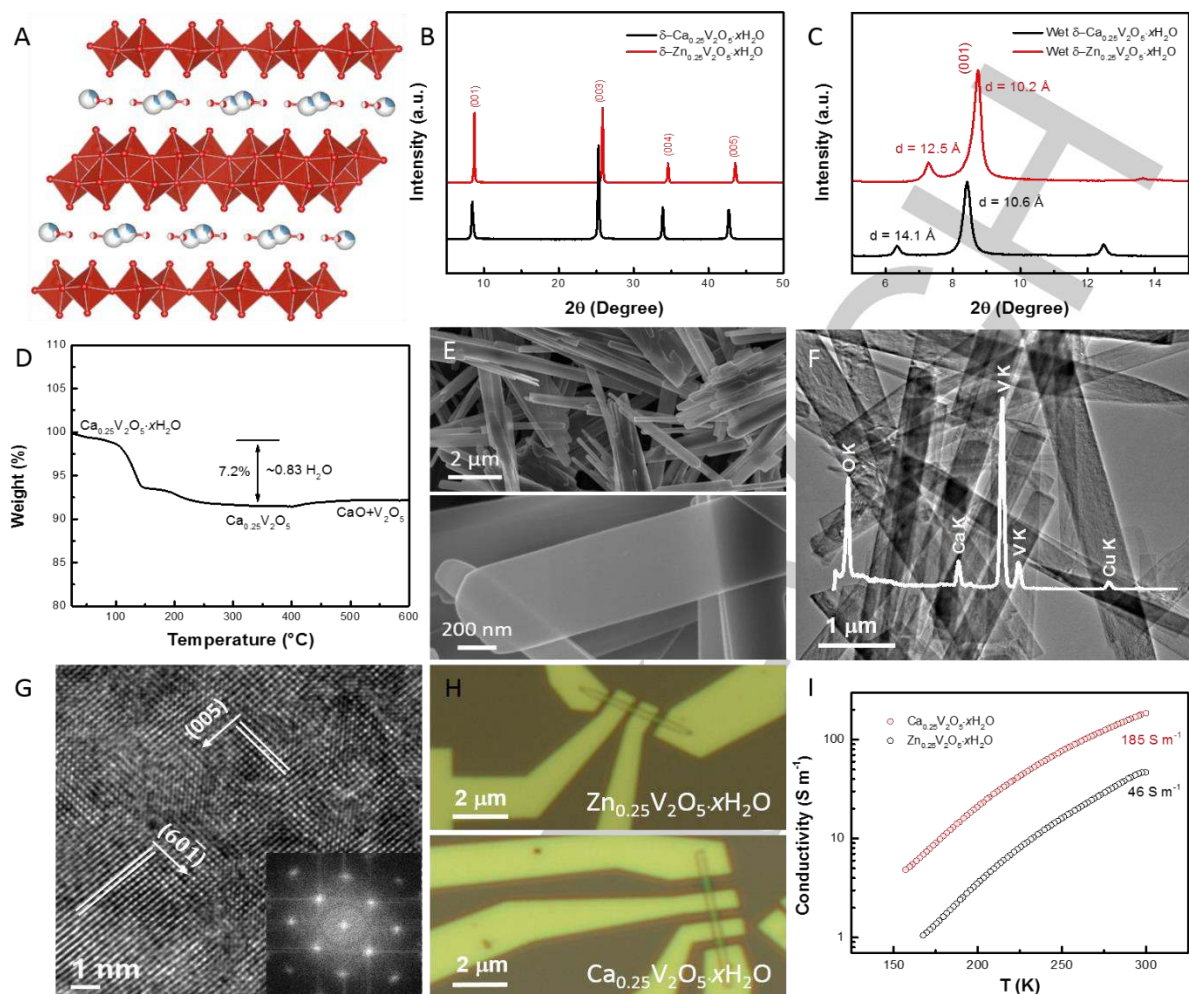


**Fig. 1.** A) Crystal structure viewed along the b-axis of CVO, which shows a double-layered structure with open-framework. The V atoms in V<sub>2</sub>O<sub>5</sub> polyhedra are depicted in red. The blue-white and red-white atoms in the crystal represent the intercalated Ca ions and lattice water, respectively. B-C) Typical XRD pattern of as-synthesized CVO. D) TGA results on CVO samples. E-G) SEM and TEM images of CVO nanobelts. Inset in (F) shows the EDS spectrum of as-obtained CVO, showing the existence of O, Ca, and V elements. The Ca/V atomic ratio is ca. 0.13. H) The individual CVO and Zn<sub>0.25</sub>V<sub>2</sub>O<sub>5</sub>·nH<sub>2</sub>O based nanodevices, and I) their corresponding electricity conductivities.

the *c* axis and the intercalated metal ions (Zn<sup>2+</sup> or Ca<sup>2+</sup>) as well as water molecules reside in the interlayer space.<sup>[12]</sup> The intercalated metal ions can strongly bond to V<sub>2</sub>O<sub>5</sub> layers and H<sub>2</sub>O to form polyhedra pillars (ZnO<sub>6</sub> and CaO<sub>7</sub>), which expand the interlayer gap of V<sub>2</sub>O<sub>5</sub> and make the formed crystal more stable. However, the Ca-O bonds in CaO<sub>7</sub> pillars (2.38~2.57 Å)<sup>[12]</sup> are much longer than Zn-O bonds (2.03~2.13 Å)<sup>[11]</sup> in Zn<sub>0.25</sub>V<sub>2</sub>O<sub>5</sub>·nH<sub>2</sub>O, implying that an increased interlayer space is expected for the CVO crystal. The XRD analysis supports our hypothesis. As displayed in **Fig. 1b**, the XRD pattern of pristine CVO is dominated by (00*l*) reflections, revealing a high degree of preferred orientation along the *c* axis. Further, the absence of any impurity peaks demonstrates the single-phase nature of as-prepared CVO. The downshift of the diffraction angle corresponding to (00*l*) peaks of CVO compared to Zn<sub>0.25</sub>V<sub>2</sub>O<sub>5</sub>·nH<sub>2</sub>O confirms its larger interlayer distance along (00*l*) direction. We also found that the V<sub>2</sub>O<sub>5</sub> open-framework of CVO allows the insertion of water molecules from the electrolyte into its interlayer space, in agreement with previous report.<sup>[2]</sup> The XRD result (**Fig. 1c**) indicates that the interlayer space of CVO increased from 10.6 to 14.1 Å upon immersion in electrolyte, corresponding to water intercalation. Of note, the

pristine XRD pattern can be recovered by vacuum drying. Apparently, more water molecules can be intercalated into CVO lattice (3.5 Å increase of interlayer space) compared to Zn<sub>0.25</sub>V<sub>2</sub>O<sub>5</sub>·nH<sub>2</sub>O (2.3 Å increase of interlayer space), confirming a more open crystal structure for CVO. This feature may facilitate the electrochemical (de)intercalation of Zn<sup>2+</sup> ions into CVO crystal. Inductively coupled plasma optical emission spectroscopy (ICP-OES) and thermogravimetric (TGA) studies (**Fig. 1d**) further reveal that the stoichiometric formula for the as-prepared calcium vanadium oxide bronze is Ca<sub>0.24</sub>V<sub>2</sub>O<sub>5</sub>·0.83H<sub>2</sub>O.

Scanning electron microscope (SEM) images reveal a typical nanobelt morphology with smooth surface of as-synthesized CVO (**Fig. 1e**), which show the nanobelts to be a few micrometers long and several hundred nanometers wide. The representative TEM images (**Fig. 1f-g**) further illustrate the flat ribbon morphology and single-crystallinity of CVO materials. A lattice fringe with d-spacing of 0.196 and 0.211 nm can be observed in the high-resolution TEM image, corresponding to (60 $\bar{1}$ ) and (005) planes of CVO nanobelt, respectively. The elemental composition of the nanobelt was investigated by energy-dispersive X-ray



## COMMUNICATION

spectroscopy (EDS) (inset in **Fig. 1f**) and the result shows that the atomic ratio of Ca to V is *ca.* 0.13, which is close to that of  $\text{Ca}_{0.24}\text{V}_2\text{O}_5 \cdot 0.83\text{H}_2\text{O}$ . Additionally, we show that the CVO nanobelts are typically 50~60 nm thick, as determined by atomic force microscopy (supporting **Fig. S2**). Considering the importance of electrical conductivity of electrode materials for energy storage applications, we then precisely measured the electrical conductivities of as-prepared samples using individual nanobelt based nanodevices (**Fig. 1h**). As shown in **Fig. 1i**, the CVO sample offers a 4-fold higher electrical conductivity than previously reported  $\text{Zn}_{0.25}\text{V}_2\text{O}_5 \cdot n\text{H}_2\text{O}$  nanobelt at room-temperature. Undoubtedly, the higher electrical conductivity can boost the electron transfer during  $\text{Zn}^{2+}$  (de)intercalation, thereby enhancing battery performance.

The freestanding CVO paper electrode was used as cathode in aqueous ZIB, where the zinc metal and 1.0 M  $\text{ZnSO}_4$  aqueous solution were used as anode and electrolyte, respectively. The CVO paper electrode ( $\approx 5.7 \text{ mg cm}^{-2}$ ) was prepared using a vacuum filtration method (see experimental section). The Zn//CVO cells were cycled in a voltage window of 0.6~1.6 V versus Zn, considering the structural stability of cathode materials. As shown in supporting **Fig. S3a**, in such a voltage window the Zn cell is very robust. Supporting **Fig. S3b** shows the 1<sup>st</sup>, 2<sup>nd</sup>, 5<sup>th</sup> and 10<sup>th</sup> cycle of the cyclic voltammetry (CV) curves at a scan rate of  $0.1 \text{ mV s}^{-1}$ . Multiple pairs of redox peaks are observed, demonstrating a multistep reaction mechanism associated with  $\text{Zn}^{2+}$  insertion/extraction. The CV study implies that the  $\text{Zn}^{2+}$  (de)intercalation process in Zn//CVO cell is highly reversible since no obvious peak current losses are observed from 2<sup>nd</sup> to 10<sup>th</sup> CV scans. **Fig. 2a** shows the galvanostatic charge-discharge (CD) profiles at various current densities. A high initial capacity of  $340 \text{ mAh g}^{-1}$  is achieved at 0.2 C. The predominantly sloping CD curves suggest fast kinetics which originate from the solid-solution type process. To further understand the electrochemical kinetics of CVO cathode, we quantified the capacitive and diffusion limited contributions to the total capacity using previously reported approach by Dunn and co-workers.<sup>[13]</sup> **Fig. 2b** exhibits the CV curves of CVO electrode from 0.2 to  $0.5 \text{ mV s}^{-1}$ . With increasing scan rates, the CV curves maintain the same shape with subtle shifting of redox peaks. The results, summarized in **Fig. 2c**, show that at a scan rate of  $0.3 \text{ mV s}^{-1}$ , 76% of the current can be attributed to the capacitive response of the CVO cathode, clearly revealing that the corresponding solid-solution reactions are mainly limited by the electrochemical reaction rate themselves instead of the mobile ion diffusion rate. Further, we employed the galvanostatic intermittent titration technique (GITT) to estimate the  $\text{Zn}^{2+}$  ion diffusion coefficient in CVO cathode (see details in supporting **Fig. S4**). Despite the divalent nature of the  $\text{Zn}^{2+}$  ion, the GITT-determined diffusion coefficient is still as high as  $\approx 10^{-8}$  to  $10^{-9} \text{ cm}^2 \text{ s}^{-1}$ . The above discussion clearly demonstrates the fast kinetics of as-prepared CVO materials, and imply their good rate capability.

The rate performance of our CVO cathode is illustrated in **Fig. 2d**, where the current density was increased step-wise from 0.2 to 80 C and returned to 0.2 C. It is obvious that the CVO electrodes retain 85% of the initial specific capacity when current increases from 0.2 ( $340 \text{ mAh g}^{-1}$ ) to 1 C ( $289 \text{ mAh g}^{-1}$ ), outperforming

previously reported  $\text{Zn}_{0.25}\text{V}_2\text{O}_5 \cdot n\text{H}_2\text{O}$  (300 and  $282 \text{ mAh g}^{-1}$  at 1/6 and 1 C, respectively). Even at a fast charge-discharge rate of 80 C (45 s), these CVO electrodes still offer a high capacity of  $72 \text{ mAh g}^{-1}$  due to the fast  $\text{Zn}^{2+}$  ion migration. Of note, the capacity of these CVO electrodes recovered to  $323 \text{ mAh g}^{-1}$  (95%) when the current density was returned to 0.2 C, suggesting excellent structural stability. We also note that the CVO cathodes do not show notable capacity decay over at least 3000 cycles ( $\approx 96\%$  retention) even at very high current density of 80 C (**Fig. 2e**). In contrast, the  $\text{Zn}_{0.25}\text{V}_2\text{O}_5 \cdot n\text{H}_2\text{O}$  cathode show 19% capacity decay only after 1000 cycles at 8 C rate.<sup>[2]</sup> It is worthwhile to note that Columbic efficiency of CVO cathode during cycling tests is close to 100%, confirming that the impressive cycling performance is not due to parasitic reactions. **Figure 2f** shows the Ragone plot of our Zn//CVO cell, in comparison to other reported intercalation Zn cells. Impressively, our devices show a very high energy density of  $267 \text{ Wh kg}^{-1}$  at a power density of  $53.4 \text{ W kg}^{-1}$ . Even when charging the cell within 45 s, the energy density is still as high as  $133 \text{ Wh kg}^{-1}$  at an outstanding power density of  $1825 \text{ W kg}^{-1}$ . Furthermore, it can be seen that our cells offer better performance than cells based on  $\text{Zn}_3\text{V}_2\text{O}_7(\text{OH})_2$ ,<sup>[14]</sup>

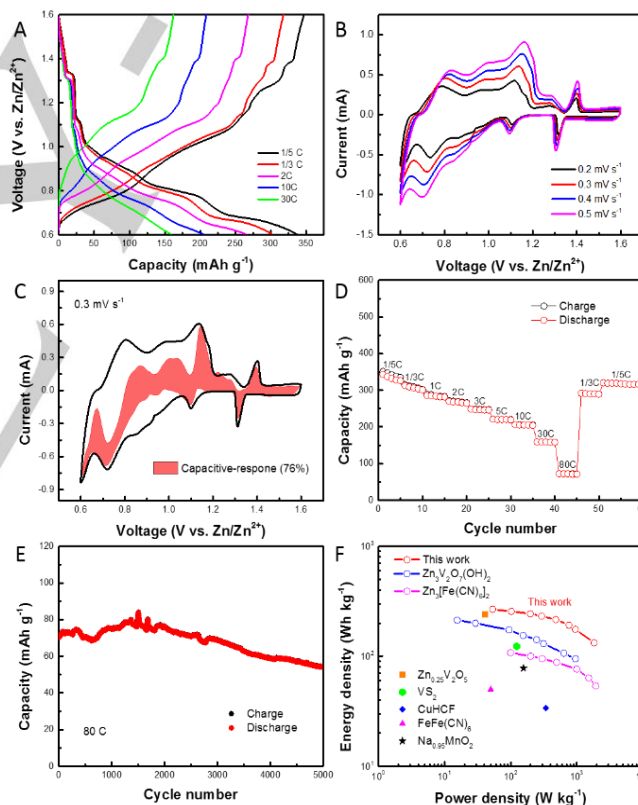


**Fig. 2.** A) Galvanostatic charge-discharge profiles for CVO electrodes at different current densities. B) Cyclic voltammetry curves of CVO electrodes at various scan rates. C) Capacity separation analysis at  $0.3 \text{ mV s}^{-1}$ . The red-shaded data show the contribution to capacitive charge storage as a function of potential. D) Rate performance of CVO cathodes. E) Cycle performance at a current rate of 80 C. F) The Ragone plot of Zn//CVO cell in comparison with other aqueous ZIBs.

$\text{Zn}_{0.25}\text{V}_2\text{O}_5 \cdot n\text{H}_2\text{O}$ ,<sup>[2]</sup>  $\text{Zn}_3[\text{Fe}(\text{CN})_6]_2$ ,<sup>[8a]</sup>  $\text{CuHCF}$ ,<sup>[8b]</sup>  $\text{VS}_2$ ,<sup>[15]</sup>  $\text{FeFe}(\text{CN})_6$ ,<sup>[16]</sup> and  $\text{Na}_{0.95}\text{MnO}_2$ ,<sup>[17]</sup> cathodes.

The successful and stable aqueous storage of  $\text{Zn}^{2+}$  in CVO cathode can be demonstrated by *ex-situ* high-resolution XPS

## COMMUNICATION

analysis. As shown in **Fig. 3a**, there is no Zn signal in the initial state for CVO cathode. However, the Zn 2p peaks ( $2p_{3/2}$ : 1022 eV)<sup>[18]</sup> emerge when the CVO electrodes were discharged to 0.6 V. The newly evolved Zn peaks clearly demonstrate the successful insertion of  $\text{Zn}^{2+}$  ions into porous CVO lattice. Next, we show that the  $\text{CaO}_7$  pillars are quite stable during  $\text{Zn}^{2+}$  incorporation. Specifically, we do not observe any intensity decrease for Ca 2p peaks as we go from initial state to fully discharged state (**Fig. 3b-c**). Further, it is worthwhile to note that

interlayer spacing of layered intercalation cathode should be expanded after guest ion incorporation. However, a small contraction (ca. 5.7%) of the CVO lattice (10.6 Å for (001) planes) is observed when discharged to 0.6 V (10 Å for (001) planes). This is likely due to increased screening of the interlayer electrostatic repulsion as the  $\text{Zn}^{2+}$  insertion and the expulsion of water molecules from the interlayer, which has been demonstrated by Nazar and co-workers.<sup>[2]</sup> Moreover, even after continuous 100 CD cycles, the CVO cathode can perfectly preserve its crystal

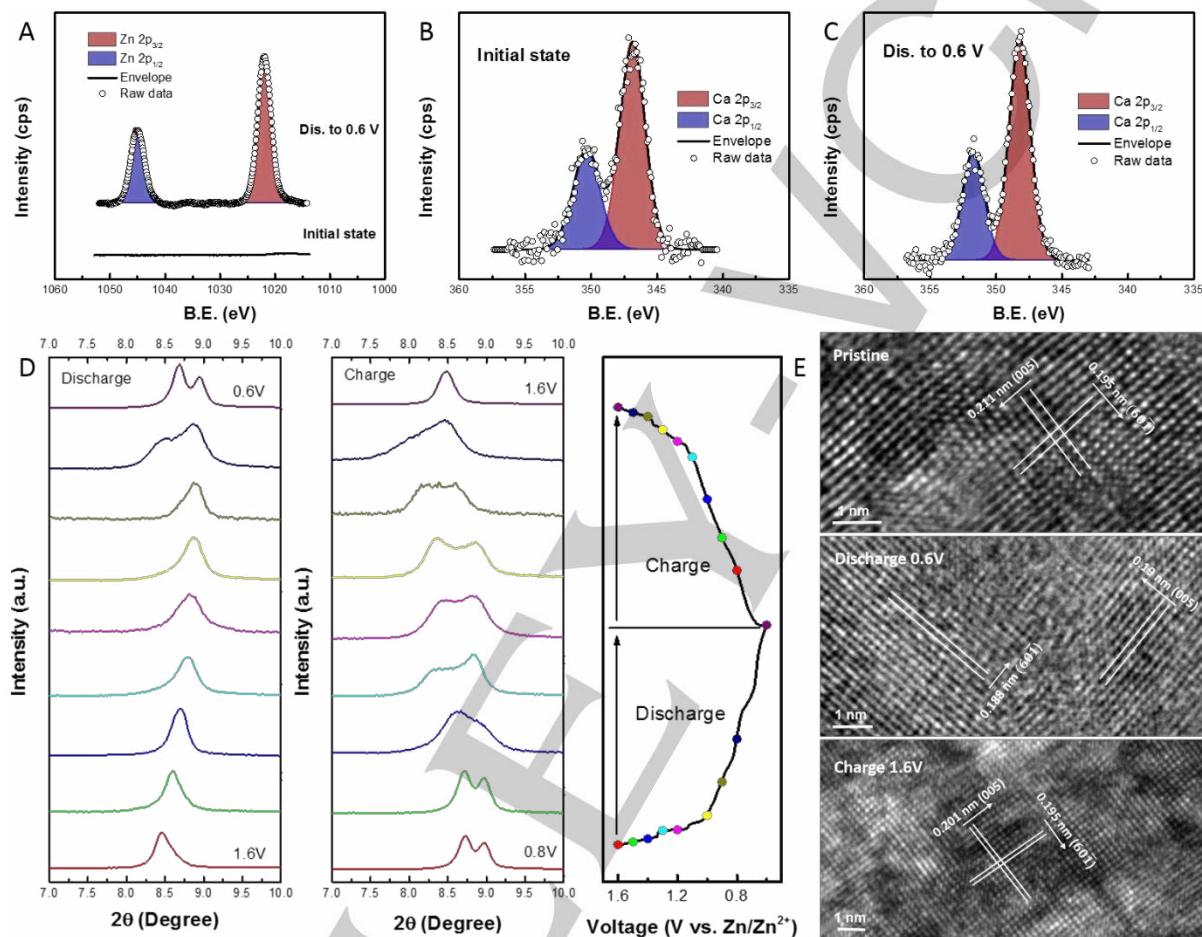


**Fig. 3.** Ex-situ high-resolution XPS spectra of the A) Zn 2p and B-C) Ca 2p regions in pristine and fully discharged state of the CVO electrodes. D) Ex-situ XRD patterns of (001) Bragg peak of the CVO cathode 3<sup>rd</sup> charge–discharge scan as a function of discharge and charge voltage. E) Ex-situ high-resolution TEM images of the CVO nanobelt at initial, fully discharged (0.6 V) and charged state (1.6 V).

fully discharged CVO electrode shows only one Ca 2p component ( $\text{Ca}^{2+}$ ), implying that the  $\text{CaO}_7$  pillars are not partially reduced as a consequence of  $\text{Zn}^{2+}/2\text{e}^-$  intercalation. The blue shift (346.9 eV for pristine CVO; 348.1 eV for discharged state) of binding energy for  $\text{Ca}^{2+}$  component in fully discharged CVO cathode is linked to the intercalation of the  $\text{Zn}^{2+}$  ions. A very similar blue shift was previously observed in Cr intercalated  $\text{CaCO}_3$  system.<sup>[19]</sup> In order to gain better insight into the electrochemical process during  $\text{Zn}^{2+}$  (de)intercalation, ex-situ XRD analysis was carried out. Supporting **Fig. S5** shows that (001) Bragg peaks corresponding to CVO phase shift to higher angles in the fully discharged state (0.6 V), and nearly return to their initial positions upon discharging to 1.6 V. Obviously, the CVO cathode does not undergo a phase evolution following  $\text{Zn}^{2+}$  insertion and extraction. Typically, the

structure without impurities formation, e.g. basic zinc sulfate. The 100 times cycled CVO electrode retained a 10.3 Å interlayer spacing, similar to the 10.6 Å interlayer spacing observed in fresh CVO nanobelt, indicating highly reversible  $\text{Zn}^{2+}$  intercalation of CVO host without structural breakdown.

**Fig. 3d** displays the evolution of the (001) peak of CVO electrode in detail during the 3<sup>rd</sup> CD scan. During the discharge process,  $\text{Zn}^{2+}$  ions are gradually intercalated into the  $\text{V}_4\text{O}_{10}$  double-layers, leading to a contraction of interlayer spacing, which can be immediately recovered upon voltage reversal. This reversibility and gradual shifting of the (001) peak indicates that the related solid-solution process is associated with  $\text{Zn}^{2+}$  (de)intercalation from CVO interlayer. We also notice that a peak split appears

## COMMUNICATION

when CVO is discharged to 0.8 V, which probably results from a dramatic crystal distortion. At 0.6 V, an obvious peak split is observed. While cycling in a wide voltage window resulted in more  $\text{Zn}^{2+}$  intercalation, the huge structural stress could lead to very fast capacity decay. Thus, 0.6 V is identified as cut-off voltage for our Zn//CVO cells. About 1.31 Zn/CVO can be intercalated into CVO lattice without apparent crystal breakdown. The *ex-situ* high-resolution TEM analysis provides further proof for the unusual  $\text{Zn}^{2+}$  storage mechanism of CVO cathodes. As shown in **Fig. 3e**, the (601) and (005) planes of pristine CVO nanobelt exhibit lattice fringes with d-spacing of 0.195 and 0.211 nm, respectively. When discharged to 0.6 V, a lattice fringe with d-spacing of 0.188 and 0.19 nm is observed, corresponding to (601) and (005) planes, respectively. Such a subtle lattice contraction (3.6-9.9%) is consistent with our XRD data. Impressively, the contracted crystal structure immediately recovered to its initial state (0.195 and 0.201 nm for (601) and (005) planes, respectively) upon  $\text{Zn}^{2+}$  ion removal (1.6 V). These findings match with those deduced from the *ex-situ* XRD and XPS studies: the CVO nanobelt is suitable cathode material for stable aqueous Zn-ion storage. Furthermore, considering the abundance and low cost of both Ca, Zn and V, our Zn//CVO cell presents a potentially safe, durable, and cost-efficient device for large-scale energy storage.

In this communication, calcium vanadium oxide bronze ( $\text{Ca}_{0.24}\text{V}_2\text{O}_5 \cdot 0.83\text{H}_2\text{O}$ ) nanostructures are synthesized using a one-step hydrothermal method, and used as aqueous ZIB cathodes. The freestanding CVO paper cathode delivers capacities of 340 and 289 mAh  $\text{g}^{-1}$  at 0.2 and 1 C, respectively. Our Zn//CVO cells show impressive energy density of 267 Wh  $\text{kg}^{-1}$  at a power density of 53.4 W  $\text{kg}^{-1}$ , outperforming most of previously reported prototypes. Excellent cycling stability (up to 5000 cycles at 80 C) and rate capability were also demonstrated. The structural evolution and electrochemical kinetics were discussed in detail. The low-cost and excellent lifespan show that nanostructured CVO is a viable cathode for aqueous Zn-ion storage.

## Acknowledgements

Research reported in this publication was supported by King Abdullah University of Science and Technology (KAUST).

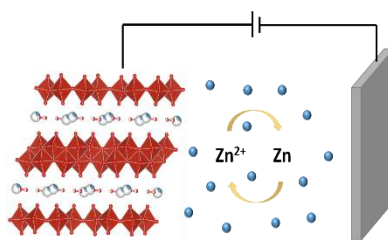
**Keywords:** calcium vanadium oxide bronze • cathode • aqueous • Zinc-ion battery • intercalation

- [1] aC. Xu, B. Li, H. Du, F. Kang, *Angewandte Chemie International Edition* **2012**, *51*, 933-935; bJ. F. Parker, C. N. Chervin, I. R. Pala, M. Machler, M. F. Burz, J. W. Long, D. R. Rolison, *Science* **2017**, *356*, 415-418; cB. J. Hertzberg, A. Huang, A. Hsieh, M. Chamoun, G. Davies, J. K. Seo, Z. Zhong, M. Croft, C. Erdonmez, Y. S. Meng, *Chem Mater* **2016**, *28*, 4536-4545.
- [2] D. Kundu, B. D. Adams, V. Duffort, S. H. Vajargah, L. F. Nazar, *Nature Energy* **2016**, *1*, 16119.
- [3] aX. Wu, Y. Cao, X. Ai, J. Qian, H. Yang, *Electrochem Commun* **2013**, *31*, 145-148; bC. D. Wessells, S. V. Peddada, R. A. Huggins, Y. Cui, *Nano Lett* **2011**, *11*, 5421-5425; cL. Peng, Y. Zhu, X. Peng, Z. Fang, W. Chu, Y. Wang, Y. Xie, Y. Li, J. J. Cha, G. Yu, *Nano Lett* **2017**, *17*, 6273-6279; dH. Li, L. Peng, Y. Zhu, D. Chen, X. Zhang, G. Yu, *Energ Environ Sci* **2016**, *9*, 3399-3405; eY. Zhu, L. Peng, D. Chen, G. Yu, *Nano Lett* **2015**, *16*, 742-747.
- [4] aX. Wu, Y. Xiang, Q. Peng, X. Wu, Y. Li, F. Tang, R. Song, Z. Liu, Z. He, X. Wu, *J Mater Chem A* **2017**, *5*, 17990-17997; bH. Zhang, K. Ye, S. Shao, X. Wang, K. Cheng, X. Xiao, G. Wang, D. Cao, *Electrochim Acta* **2017**, *229*, 371-379; cS. Liu, J. Hu, N. Yan, G. Pan, G. Li, X. Gao, *Energ Environ Sci* **2012**, *5*, 9743-9746.
- [5] G. Li, Z. Yang, Y. Jiang, C. Jin, W. Huang, X. Ding, Y. Huang, *Nano Energy* **2016**, *25*, 211-217.
- [6] M. Yan, P. He, Y. Chen, S. Wang, Q. Wei, K. Zhao, X. Xu, Q. An, Y. Shuang, Y. Shao, *Adv Mater* **2017**, 1703725.
- [7] aH. Pan, Y. Shao, P. Yan, Y. Cheng, K. S. Han, Z. Nie, C. Wang, J. Yang, X. Li, P. Bhattacharya, *Nature Energy* **2016**, *1*, 16039; bM. H. Alfaruqi, V. Mathew, J. Gim, S. Kim, J. Song, J. P. Baboo, S. H. Choi, J. Kim, *Chem Mater* **2015**, *27*, 3609-3620.
- [8] aL. Zhang, L. Chen, X. Zhou, Z. Liu, *Adv Energy Mater* **2015**, *5*, 1400930; bR. Trócoli, F. La Mantia, *Chemsuschem* **2015**, *8*, 481-485; cZ. Jia, B. Wang, Y. Wang, *Mater Chem Phys* **2015**, *149*, 601-606.
- [9] Y. Ma, H. Zhou, S. Zhang, S. Gu, X. Cao, S. Bao, H. Yao, S. Ji, P. Jin, *Chem-Eur J* **2017** DOI: 10.1002/chem.201702814.
- [10] E. Levi, Y. Gofer, D. Aurbach, *Chem Mater* **2009**, *22*, 860-868.
- [11] Y. Oka, O. Tamada, T. Yao, N. Yamamoto, *J Solid State Chem* **1996**, *126*, 65-73.
- [12] Y. Oka, T. Yao, N. Yamamoto, *J Solid State Chem* **1997**, *132*, 323-329.
- [13] J. Wang, J. Polleux, J. Lim, B. Dunn, *The Journal of Physical Chemistry C* **2007**, *111*, 14925-14931.
- [14] C. Xia, J. Guo, Y. Lei, H. Liang, C. Zhao, H. N. Alshareef, *Adv Mater* **2018**, *30*, 1705580.
- [15] P. He, M. Yan, G. Zhang, R. Sun, L. Chen, Q. An, L. Mai, *Adv Energy Mater* **2017**, *7*, 1601920.
- [16] Z. Liu, P. Bertram, F. Endres, *J Solid State Electr* **2017**, 1-7.
- [17] B. Zhang, Y. Liu, X. Wu, Y. Yang, Z. Chang, Z. Wen, Y. Wu, *Chem Commun* **2014**, *50*, 1209-1211.
- [18] S. Jeong, J. Boo, *Thin Solid Films* **2004**, *447*, 105-110.
- [19] A. Garcia-Sánchez, E. Alvarez-Ayuso, *Miner Eng* **2002**, *15*, 539-547.

## COMMUNICATION

## COMMUNICATION

**Layered calcium vanadium oxide bronze** was synthesized for aqueous zinc-ion battery applications. We demonstrate that the calcium based bronze shows promising performance for  $\text{Zn}^{2+}$  storage in aqueous electrolyte. The Zn cell delivers an energy density of  $267 \text{ Wh kg}^{-1}$  at a power density of  $53.4 \text{ W kg}^{-1}$ .



Chuan Xia, Jing Guo, Peng Li, Xixiang Zhang and Husam Alshareef\*

Page No. – Page No.

Highly Stable Aqueous Zinc-ion  
Storage Using Layered Calcium  
Vanadium Oxide Bronze Cathode